

Tunneling-induced coherent electron population transfer in an asymmetric quantum well

Ni Cui,^{1,2} Yueping Niu,^{1,*} and Shangqing Gong^{1,†}

¹*State Key Laboratory of High Field Laser Physics,
Shanghai Institute of Optics and Fine Mechanics,
Chinese Academy of Sciences, Shanghai 201800, China*

²*Graduate University of Chinese Academy of Sciences, Beijing 100049, China*

(Dated: September 7, 2018)

We propose an asymmetric double quantum well structure with a common continuum and investigate the effect of resonant tunneling on the control of coherent electron population transfer between the two quantum wells. By numerically solving the motion equations of element moments, the almost complete electron population transfer from initial subband to the target subband could be realized due to the constructive interference via flexibly adjusting the structure parameters.

PACS numbers: 78.67.De, 42.50.Hz, 73.63.-b

I. INTRODUCTION

Coherent population transfer among discrete quantum states in atoms and molecules has attracted tremendous attentions[1, 2] over the past decades, due to its potential application to atomic optics[3], preparation of entanglement[4] and quantum computation[5]. The most robust technique for achieving efficient population transfer is stimulated Raman adiabatic passage (STIRAP)[1, 2, 6], by which perfect population transfer has been studied in a three-level Λ system particularly. Moreover, the case when the upper isolated discrete level is replaced with a continuum was suggested initially by Carroll and Hioe[7]. In their model, the continuum could serve as an intermediary for population transfer between two discrete states in an atom or a molecule by STIRAP. However, complete population transfer is unrealistic, significant partial transfer may still be feasible[8, 9].

Recently, there is great interest in extending these studies to semiconductor nanostructures[10, 11, 12, 13] for the possible implementation of optoelectronic devices. In the conduction band of semiconductor quantum structure, the confined electron gas exhibits atomiclike behaviors. The intersubband energies and electron wave function symmetries could be engineered, with a flexibility unknown in atomic systems, to suit particular requirements. Therefore, several quantum optical coherence and interference effects have been investigated within intersubband transitions of semiconductor quantum wells(QWs), such as electromagnetically induced transparency(EIT)[14], tunneling-induced transparency[15], enhancement of Kerr nonlinearity[16, 17], ultrafast all-optical switching[18], four-wave mixing[19], Rabi oscillations[20], and coherent population trapping(CPT)[21].

In the present paper, we design a n-doped asymmetric AlGaAs/GaAs double QW with a continuum(Fig. 1), which has four conduction subbands with a closely separated excited doublet. It is well known that, for an excited-doublet four-level atom system, the quantum interference effect can lead to depression or even cancellation of spontaneous emission from the excited doublet to the lower levels[22, 23, 24]. Considering above, some of us[25] demonstrated that a complete population transfer from an initial state to another target state and an arbitrary superposition of atomic states could be realized with the STIRAP technique. However, the spontaneous decay is intrinsically incoherent in nature and detrimental to coherent population transfer, Zhu *et al.*[26] investigated that the remarkable enhancement or suppression of population transfer can be realized through the spontaneous emission constructive or destructive quantum interference even with a finite pulse area. In contrast to the excited-doublet four-level atom, in our structure, the quantum tunneling to a continuum from the excited doublet could give rise to the Fano-type interference[27], which has been observed experimentally in semiconductor intersubband transitions[28] and the sign of quantum interference (constructive or destructive) in optical absorption can be reversed by varying the direction of tunneling from the excited doublet to a common continuum[29]. Therefore, in the present paper, we will analyze the controllability of the coherent electron population transfer in the four-subband double QW structure via tuning the sign of quantum interference due to resonant tunneling, the splitting of the excited doublet (the coupling strength of the tunneling), and the Fano-type interference. By numerically solving the motion equations of element moments, the almost complete electron population transfer between QWs could be realized due to the constructive interference by suitably adjusting the structure parameters.

*Corresponding author. E-mail: niuyp@mail.siom.ac.cn

†Corresponding author. E-mail: sqgong@mail.siom.ac.cn

II. THE MODEL AND BASIC EQUATIONS

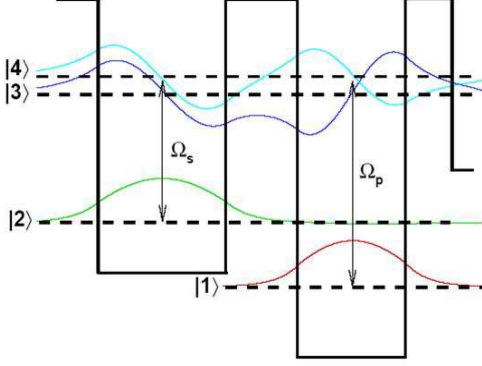


FIG. 1: Conduction subbands of the asymmetric double QW. It consists of two wells and a collector region separated by thin tunneling barriers. The dash lines denote the energy subbands and the solid curves represent the corresponding wave functions.

The n -doped asymmetric GaAs/AlGaAs double QW under consideration is shown in Fig. 1. One $\text{Al}_{0.07}\text{Ga}_{0.93}\text{As}$ QW with thickness of 8.3 nm is separated from a 6.9 nm GaAs QW by a 4.8 nm $\text{Al}_{0.32}\text{Ga}_{0.68}\text{As}$ potential barrier. On the right side of right well is a 3.4 nm thin $\text{Al}_{0.32}\text{Ga}_{0.68}\text{As}$ barrier, which is followed by a thick $\text{Al}_{0.16}\text{Ga}_{0.84}\text{As}$ layer. In this structure, the energies of the ground subbands |1> and |2> for the two wells are obtained as 51.53 meV and 97.78 meV, respectively. Two closely spaced delocalized upper levels |3> and |4>, with the energies 191.30 meV and 203.06 meV respectively, are created by mixing the first excited subband of the shallow well $|se\rangle$ and the first excited subband of the right deep well $|de\rangle$ by tunneling. The dash lines denote the energy subbands and the solid curves represent the corresponding wave functions. The subband |1> and subbands |3> and |4> are coupled by the pump laser (the amplitude E_p and center frequency ω_p) with the Rabi frequencies $\Omega_p = \mu_{13}E_p/\hbar$ and $k\Omega_p = \mu_{14}E_p/\hbar$, respectively. The subband |2> and subbands |3> and |4> are coupled by the Stokes laser (the amplitude E_s and center frequency ω_s) with the Rabi frequencies $\Omega_s = \mu_{23}E_s/\hbar$ and $q\Omega_s = \mu_{24}E_s/\hbar$, respectively. The Rabi frequencies of the pump and Stokes pulses are assumed to be Gaussian shape with the amplitude envelopes of the form $\Omega_p = \Omega_{p0} \exp[-(t - T_p)^2/\tau^2]$ and $\Omega_s = \Omega_{s0} \exp[-(t - T_s)^2/\tau^2]$, respectively, where τ is the pulse duration, and $T_p(T_s)$ is the time delay of pump (Stokes) pulse. Moreover, Ω_{p0} and Ω_{s0} are the peak values of the Rabi frequencies of pump and Stokes pulses, respectively. For simplicity, we denote $\Omega_{p0} = \Omega_{s0}$ in the following discussion. In addition, $k = \mu_{14}/\mu_{13}$ and $q = \mu_{24}/\mu_{23}$ present the ratios between the inter-subband dipole moments of the relevant transitions, and $\mu_{ij}(i, j = 1 - 4, i \neq j) = \vec{\mu}_{ij} \cdot \vec{e}_L$ (\vec{e}_L is the unit polarization vector of the corresponding laser field) denotes the dipole moment for the transition between subbands

$|i\rangle$ and $|j\rangle$. In our structure, the dipole moments ratios could be calculated to be $k = -0.70$ and $q = 0.90$.

In the four-subband QW structure, the direct optical resonance $|1\rangle(|2\rangle) \rightarrow |c\rangle$ ($|c\rangle$ is the continuum subband) is much weaker than those mediate resonance paths $|3\rangle(|4\rangle) \rightarrow |1\rangle$ and $|3\rangle(|4\rangle) \rightarrow |2\rangle$, thus the influence of the direct transition $|1\rangle(|2\rangle) \rightarrow |c\rangle$ could be ignored[27]. In addition, when the electron sheet density smaller than 10^{12} cm^{-2} and with the actual temperature at 10 K, the electron-electron effects have very small influence in our results. Under these assumptions, following the standard processes[30], the system dynamics could be described by the motion equations for the matrix elements in a rotating frame:

$$\begin{aligned} \dot{\rho}_{11} &= ik\Omega_p(\rho_{41} - \rho_{14}) + i\Omega_p(\rho_{31} - \rho_{13}) + \gamma_{41}\rho_{44} \\ &\quad + \gamma_{31}\rho_{33} + \gamma_2\rho_{22} + \frac{\eta}{2}(\rho_{34} + \rho_{43}), \end{aligned} \quad (1)$$

$$\begin{aligned} \dot{\rho}_{22} &= iq\Omega_s(\rho_{42} - \rho_{24}) + i\Omega_s(\rho_{32} - \rho_{23}) + \gamma_{42}\rho_{44} \\ &\quad + \gamma_{32}\rho_{33} - \gamma_2\rho_{22} + \frac{\eta}{2}(\rho_{34} + \rho_{43}), \end{aligned} \quad (2)$$

$$\begin{aligned} \dot{\rho}_{33} &= i\Omega_p(\rho_{13} - \rho_{31}) + i\Omega_s(\rho_{23} - \rho_{32}) - \gamma_3\rho_{33} \\ &\quad - \frac{\eta}{2}(\rho_{34} + \rho_{43}) \end{aligned} \quad (3)$$

$$\begin{aligned} \dot{\rho}_{44} &= ik\Omega_p(\rho_{14} - \rho_{41}) + iq\Omega_s(\rho_{24} - \rho_{42}) - \gamma_4\rho_{44} \\ &\quad - \frac{\eta}{2}(\rho_{34} + \rho_{43}) \end{aligned} \quad (4)$$

$$\begin{aligned} \dot{\rho}_{12} &= -[i(\Delta_p - \Delta_s) + \frac{\Gamma_{12}}{2}]\rho_{12} \\ &\quad + ik\Omega_p\rho_{42} + i\Omega_p\rho_{32} - iq\Omega_s\rho_{14} - i\Omega_s\rho_{13} \end{aligned} \quad (5)$$

$$\begin{aligned} \dot{\rho}_{13} &= -(i\Delta_p + \frac{\Gamma_{13}}{2})\rho_{13} + ik\Omega_p\rho_{43} - i\Omega_s\rho_{12} \\ &\quad + i\Omega_p(\rho_{33} - \rho_{11}) - \frac{\eta}{2}\rho_{14} \end{aligned} \quad (6)$$

$$\begin{aligned} \dot{\rho}_{14} &= -[i(\Delta_p - \omega_{43}) + \frac{\Gamma_{14}}{2}]\rho_{14} + i\Omega_p\rho_{34} \\ &\quad - iq\Omega_s\rho_{12} + ik\Omega_p(\rho_{44} - \rho_{11}) - \frac{\eta}{2}\rho_{13} \end{aligned} \quad (7)$$

$$\begin{aligned} \dot{\rho}_{23} &= -(i\Delta_s + \frac{\Gamma_{23}}{2})\rho_{23} - i\Omega_p\rho_{21} + iq\Omega_s\rho_{43} \\ &\quad + i\Omega_s(\rho_{33} - \rho_{22}) - \frac{\eta}{2}\rho_{24} \end{aligned} \quad (8)$$

$$\begin{aligned} \dot{\rho}_{24} &= -[i(\Delta_s - \omega_{43}) + \frac{\Gamma_{24}}{2}]\rho_{24} - ik\Omega_p\rho_{21} \\ &\quad + i\Omega_s\rho_{34} - iq\Omega_s(\rho_{22} - \rho_{44}) - \frac{\eta}{2}\rho_{23} \end{aligned} \quad (9)$$

$$\begin{aligned} \dot{\rho}_{34} &= -(-i\omega_{43} + \frac{\Gamma_{34}}{2})\rho_{34} - ik\Omega_p\rho_{31} + i\Omega_p\rho_{14} \\ &\quad - iq\Omega_s\rho_{32} + i\Omega_s\rho_{24} - \frac{\eta}{2}(\rho_{33} + \rho_{44}) \end{aligned} \quad (10)$$

with $\rho_{ij} = \rho_{ji}^*$ and the electron conservation condition $\rho_{11} + \rho_{22} + \rho_{33} + \rho_{44} = 1$. Here, $\omega_{ij}(i, j = 1 - 4, i \neq j) = \omega_i - \omega_j$ is the resonant frequency between subbands $|i\rangle$ and $|j\rangle$, and $\omega_i(i = 1 - 4)$ is the frequency of the subband $|i\rangle$. $\omega_{43} = \omega_4 - \omega_3$ is the energy splitting between levels |4> and |3>, given by the coherent coupling strength of the electron tunneling. $\Delta_p = \omega_p - \omega_{31}$ is the

detuning of the pump laser from the resonant transition $|1\rangle \rightarrow |3\rangle$, and $\Delta_s = \omega_s - \omega_{32}$ is the detuning between the frequency of the Stokes laser and the transition frequency ω_{32} . The population decay rates and dephasing decay rates are added phenomenologically in the above density-matrix. The population decay rates for subband $|i\rangle$ denoted by γ_i , are due primarily to longitudinal-optical (LO) phonon emission events at low temperature. The total decay rates ($\Gamma_{ij}(i \neq j)$) are given by $\Gamma_{12} = \gamma_2 + \gamma_{12}^{dph}$, $\Gamma_{13} = \gamma_3 + \gamma_{13}^{dph}$ ($\gamma_3 = \gamma_{31} + \gamma_{32}$), $\Gamma_{14} = \gamma_4 + \gamma_{14}^{dph}$ ($\gamma_4 = \gamma_{41} + \gamma_{42}$), $\Gamma_{23} = \gamma_2 + \gamma_3 + \gamma_{23}^{dph}$, $\Gamma_{24} = \gamma_2 + \gamma_4 + \gamma_{24}^{dph}$, $\Gamma_{34} = \gamma_3 + \gamma_4 + \gamma_{34}^{dph}$, where the pure dephasing decay rate γ_{ij}^{dph} is determined by electron-electron effects, interface roughness, and phonon scattering process. For temperature up to 10 K with electron sheet densities smaller than 10^{12} cm^{-2} , the dephasing rates could be estimated[15] to be $\gamma_{13}^{dph} = \gamma_{23}^{dph} = 0.32 \text{ meV}$, $\gamma_{14}^{dph} = \gamma_{24}^{dph} = 0.30 \text{ meV}$, $\gamma_{34}^{dph} = 0.31 \text{ meV}$ and $\gamma_{12}^{dph} = 0.47 \times 10^{-9} \text{ meV}$. For our QWs considered, the population decay rates turn out to be $\gamma_3 = 1.58 \text{ meV}$, $\gamma_4 = 1.50 \text{ meV}$, and $\gamma_2 = 2.36 \times 10^{-9} \text{ meV}$.

The Fano interference factor $\eta = \sqrt{\gamma_3 \gamma_4}$ represents the mutual coupling of subbands $|3\rangle$ and $|4\rangle$ arising from the tunneling to the continuum through the thin barrier. We define $\epsilon = \eta / \sqrt{\Gamma_{13} \Gamma_{14}}$ for assessing the strength of the cross coupling, where the limit values $\epsilon = 0$ and $\epsilon = 1$ correspond to no interference (negligible coupling between $|3\rangle$ and $|4\rangle$) and perfect interference (no dephasing), respectively. From the above estimates, we obtain $\epsilon = 0.83$, which could be augmented by decreasing the temperature which generally leads to smaller dephasing γ_{ij}^{dph} .

III. THE COHERENT ELECTRON POPULATION TRANSFER

In this section, we will investigate the achievement of perfect coherent electron population transfer in an asymmetric semiconductor QW system interacting with a counterintuitively ordered pulses (i.e., the Stokes pulse precedes the pump pulse), by properly adjusting the QW structure parameters, such as the sign of quantum interference due to resonance tunneling, the splitting of the excited doublet (the coupling strength of the tunneling), as well as the coupling strength of Fano-type interference.

Without the consideration of the electron dephasing and population decays of the excited doublet, the four-subband QW structure is similar to the excited-doublet four-level atom system [24, 25, 26], in which some[25] of us have demonstrate that the dark states could exist with the contribution from the excited doublet, and the behavior of adiabatic passage depends crucially on the detunings between the laser frequencies and the atomic transition frequency. When the pump and Stokes fields keep two-photon resonance, but are not tuned at the midpoint of the excited doublet, only one dark state exists,

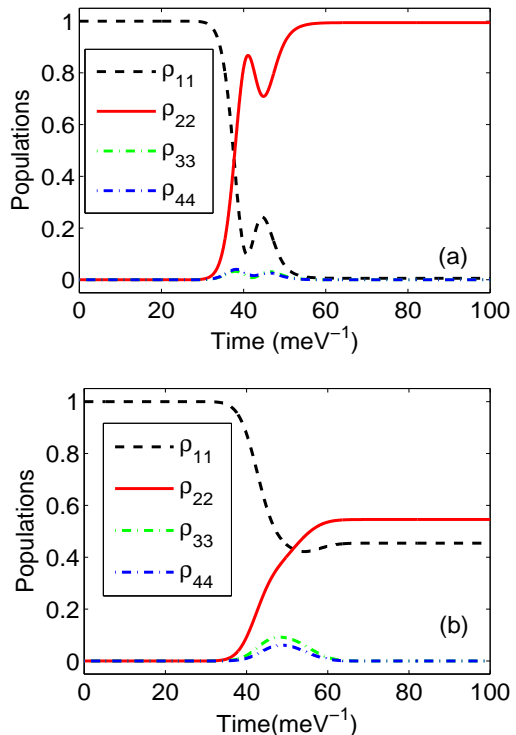


FIG. 2: The time evolution of the populations in the four subbands ρ_{11} (dash line), ρ_{22} (solid line), ρ_{33} (dot-dash line) and ρ_{44} (dash-dot line) with the laser fields tuned at the middle point of the upper two subbands under different values of the dipole ratios $k = -0.70$ and $q = 0.90$ in (a), and $k = 0.70$ and $q = 0.90$ in (b) with $\Omega_{p0} = \Omega_{s0} = 2.6 \text{ meV}$, $\tau = 10 \text{ meV}^{-1}$, $T_s = 30 \text{ meV}^{-1}$, $T_p = 50 \text{ meV}^{-1}$, $\omega_{43} = 11.76 \text{ meV}$, $\gamma_3 = 1.58 \text{ meV}$, $\gamma_4 = 1.50 \text{ meV}$ and $\gamma_2 = 2.36 \times 10^{-9} \text{ meV}$.

which is

$$|\phi_0\rangle = \cos \theta |1\rangle - \sin \theta |2\rangle, \quad (11)$$

where $\tan \theta = \Omega_p / \Omega_s$, and θ is the mixing angle used in standard STIRAP. In the adiabatic regime, a complete population transfer from an initial state $|1\rangle$ to another target state $|2\rangle$ can be realized with counterintuitively ordered pulses, just as in the three-level Λ system[1]. However, when both pump and Stokes fields are tuned to the center of the two upper levels, there exist two dark states, one is the trapped state of Eq. (11), and the other is

$$|\phi_1\rangle = \sin \theta \sin \varphi |1\rangle + \cos \theta \sin \varphi |2\rangle + \frac{\cos \varphi}{\sqrt{2}} (|3\rangle - |4\rangle), \quad (12)$$

where $\tan \varphi = \omega_{43} / 2 / \sqrt{2 [\Omega_s^2 + \Omega_p^2]}$, and φ is an additional mixing angle related to the energy separation of the excited doublet. For a counterintuitively ordered pulses, due to the nonadiabatic coupling between the two degenerate states ϕ_0 and ϕ_1 , the system vector $\Psi(\infty)$ is a mixture of the two bare states $|1\rangle$ and $|2\rangle$, as follows

$$|\Psi(\infty)\rangle = \sin \gamma_f(\infty) |1\rangle - \cos \gamma_f(\infty) |2\rangle, \quad (13)$$

where $\gamma_f = \int_{-\infty}^t (d\theta/dt') \sin \varphi dt'$ is the Berry phase[25]. Obviously, an arbitrary superposition of atomic states can be prepared when ω_{43} is comparable to Ω_p and Ω_s . It can also be seen from Eq. (13) that, if ω_{43} is much larger than Ω_p and Ω_s , then φ nearly equals $\pi/2$, and almost no population transfer can occur; while if the energy separation of the doublet ω_{43} is far smaller than the peak Rabi frequencies Ω_p and Ω_s , then φ is nearly equal to zero, and the population transfer behaves almost in the same manner as that in the Λ -type three-level system.

It should be emphasized that the results obtained in Ref. [25] are based on the relationship $\frac{\Omega_p}{k\Omega_p} = \frac{\Omega_s}{q\Omega_s}$, which means $k = q$. Indeed, the condition $k = q$ could be approximately fulfilled, when we design the asymmetric double QWs with the continuum adjacent to the shallow well, under which both wave functions of subbands $|3\rangle$ and $|4\rangle$ are symmetric[29]. However, the coherent population transfer could be suppressed due to the destructive interference when the dephasing and population decays of the excited doublet are taken into account[Fig. 2(b)], as analyzed in Ref. [26] within the excited doublet four-level atomic system with spontaneous decay-induced coherence. In our structure, we design an asymmetric QW with the continuum adjacent to the deep well, owing to resonant tunneling, the wave functions of subbands $|3\rangle$ and $|4\rangle$ are symmetric and asymmetric combinations of $|se\rangle$ and $|de\rangle$ (see Fig. 1). As a result, $kq < 0$, i.e., the relationship $k = q$ can't be held. When the pump and Stokes fields keep two-photon resonance, no dark states exist in our structure. However, when the electron dephasing and population decays of the excited doublet are taken into account, the almost complete electron population transfer from an initial subband to another target subband could be realized due to the constructive interference from resonance tunneling with a finite pulse area.

By numerically solving the density matrix equations [Eqs. (1)-(10)], we will investigate the effects of the sign of resonance tunneling on the electron population transfer in a four-subband quantum well structure with a continuum adjacent to the deep or shallow well. Figure. 2(a) presents the time evolution of the populations in the four subbands of QWs [Fig. 1] with the element ratios $k = -0.70$ and $q = 0.90$, for the pump and Stokes fields keeping the two-photon resonance and tuned midway between the excited doublet $|3\rangle$ and $|4\rangle$. The fields parameters are taken as $\Omega_{p0} = \Omega_{s0} = 2.6$ meV, $\tau = 10$ meV $^{-1}$, $T_s = 30$ meV $^{-1}$, and $T_p = 50$ meV $^{-1}$, and the Rabi frequency is quite smaller than the energy splitting of the excited doublet $\omega_{43} = 11.76$ meV. For comparison, Figure. 2(b) gives the time evolution of the populations in four-subband QWs with the continuum adjacent to the shallow well, which is similar to that in Fig.1b in Ref. [29], with the element ratios $k = 0.70$ and $q = 0.90$. It can be seen that the electron population transfer is dramatically modified by the sign of the interference(destructive or constructive) due to resonant tunneling. In the case of $k = 0.70$ and $q = 0.90$, in which the dipole moments be-

tween the two upper subbands and each of the two lower subbands are parallel, only a part of populations can be transferred from subband $|1\rangle$ to subband $|2\rangle$ [Fig. 2(b)]. This phenomenon is due to the destructive interference via spontaneous decay pathways which prevents the electron population in subband $|1\rangle$ from being excited by the pump field. That is to say, the asymmetric QW structure with the continuum adjacent to the shallow well is not suitable for the investigation of electron population transfer with the pump and Stokes fields tuned midway between the excited doublet. However, in contrast, by constructing the continuum adjacent to the deep well through the thin barrier(see in Fig. 1), the sign of the transition matrix element changes as $k = -0.70$, and $q = 0.90$. When the pump and Stokes fields keep the two-photon resonance and are tuned at the center of the excited doublet, an almost complete electron population transfer could be realized due to the constructive interference via resonant tunneling which suppresses the effects of the quantum coherence of spontaneous decays, as shown in Fig. 2(a). Therefore, the perfect electron population transfer could be achieved by suitably modulating the sign of the interference induced by resonant tunneling, which could be obtained by varying the direction of tunneling from the excited doublet to a common continuum[29].

Then, we analyze how the energy splitting of the excited doublet, which is given by the coupling strength of the tunneling, effects the electron population transfer behavior. For our structure, the splitting on resonance is given by the coupling strength and could be controlled by adjusting the height and width of the tunneling barrier. While keeping other parameters fixed except the width of the tunneling barrier between different quantum wells, we present the time evolution of the populations in the four subbands with different splittings of the excited doublet in Fig. 3. Compared with Fig. 2(a), it is can be seen that, the perfect electron population transfer occurs when the splitting ω_{43} is much smaller [$\omega_{43} = 5.93$ meV in Fig. 3(a)]. As further decreasing the splitting [even smaller than the peak Rabi frequencies Ω_p and Ω_s], the electron populations could also be completely transferred from the initial subband $|1\rangle$ to the target subband $|2\rangle$, which is not shown here. While with increasing the splitting of the excited doublet, the electron population transfer becomes lower, such as $\omega_{43} = 25.38$ meV in Fig. 3(b). The results are in accordance with the analysis from Eq. (13), which could also be well understood from the final populations as a function of the one-photon resonance satisfied under different values of the splittings of excited doublet, as shown in Fig. 4.

From Fig. 4, we find that nearly complete electron population transfer from the initial subband $|1\rangle$ to the target subband $|2\rangle$ at the middle point of the two one-photon resonances with smaller splitting of excited doublet [$\omega_{43} = 5.93$ meV in Fig. 4(a) and $\omega_{43} = 11.76$ meV in Fig. 4(b)]. As the energy splitting of the excited doublet are much larger than the laser field Rabi frequency

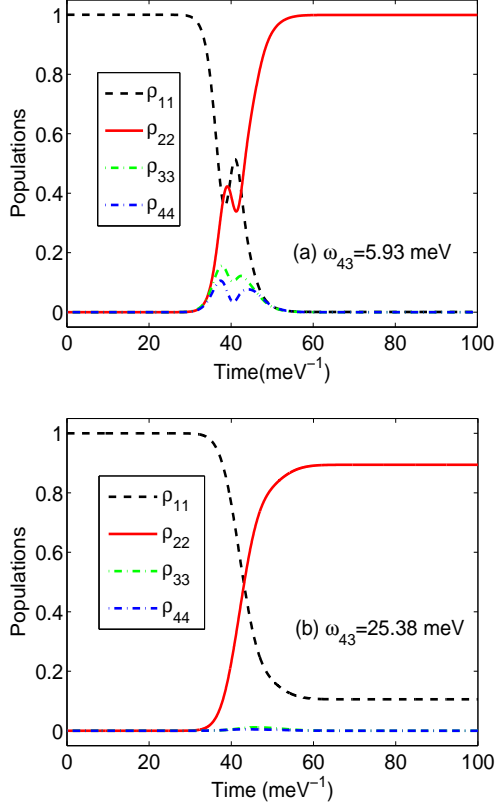


FIG. 3: The time evolution of the populations in the four subbands ρ_{11} (dash line), ρ_{22} (solid line), ρ_{33} (dot-dash line) and ρ_{44} (dot-dash line) with the laser fields tuned at the middle point of the upper two subbands under different splittings of the doublet, (a) $\omega_{43} = 5.93$ meV, $k = -0.59$ and $q = 1.20$, (b) $\omega_{43} = 25.38$ meV, $k = -0.61$ and $q = 0.56$. The other parameters are the same as in Fig. 2(a).

[$\omega_{43} = 25.38$ meV], the electron population transfer efficiency at the middle point decreases with the limited pulse area. Therefore, the almost complete electron population transfer could be controlled simply by adjusting the energy splitting of the excited doublet, i.e., the width or the height of the tunneling barrier. Therefore, the almost electron population transfer to a target subband in QWs could be controlled by appropriately adjusting the tunneling barrier.

In addition, the effects of the strength or quality of the Fano-type interference on electron population transfer behavior could be clearly seen from Fig. 5. From this figure, we can see that the population transfer efficiency increases as the strength of interference ε increasing. The reason is that, the increase of the strength of the interference, which means the decrease of the dephasing process, enhances the coherence from the constructive quantum interference. As a result, we can achieve an almost complete electron population transfer via properly increasing the Fano interference, which could be achieved by decreasing the temperature.

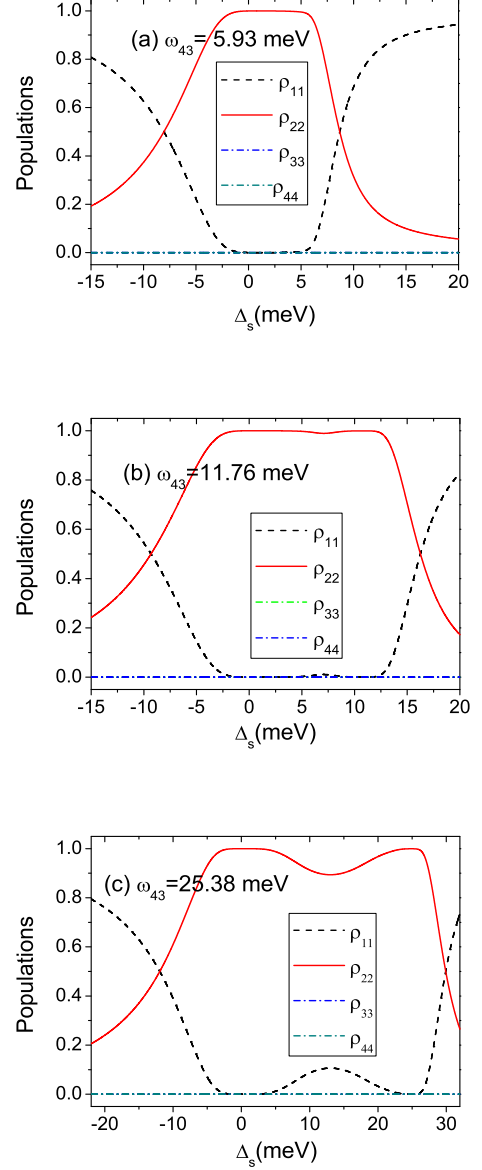


FIG. 4: The final populations in the four subbands ρ_{11} (dash line), ρ_{22} (solid line), ρ_{33} (dot-dash line) and ρ_{44} (dot-dash line) as a function of the one-photon detunings of the pump and Stokes lasers $\Delta_p = \Delta_s$, with different splittings of the doublet, (a) $\omega_{43} = 5.93$ meV, $k = -0.59$ and $q = 1.20$, (b) $\omega_{43} = 11.76$ meV, $k = -0.70$ and $q = 0.90$, (c) $\omega_{43} = 25.38$ meV, $k = -0.61$ and $q = 0.56$. The other parameters are the same as in Fig. 2(a).

It should be noted that a change in the splitting of excited doublet may be connected to a slight change in dephasing and decay rates. However, via properly adjusting other physical variables such as temperatures, interface roughness scattering and so on, we believe that some experimental scientists have adequate wisdom to keep them unchanged. As a matter of fact,

IV. CONCLUSIONS

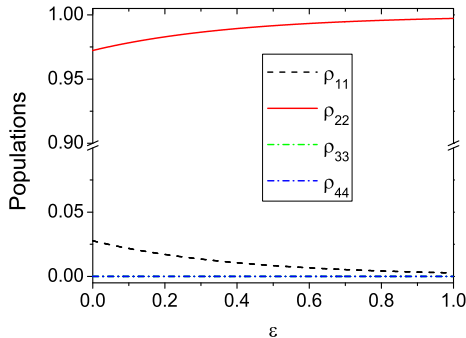


FIG. 5: The final populations in the four subbands ρ_{11} (dash line), ρ_{22} (solid line), ρ_{33} (dot-dash line) and ρ_{44} (dot-dash line) as a function of the Fano interference factor ε . The other parameters are the same as in Fig. 2(a).

we have tried several other values of dephasing rates $\gamma_{12}^{dph}, \gamma_{13}^{dph}, \gamma_{14}^{dph}, \gamma_{23}^{dph}, \gamma_{24}^{dph}, \gamma_{34}^{dph}$, and population decay rates $\gamma_2, \gamma_3, \gamma_4$ with the changes of the splitting of the excited doublet, similar coherent population transfer behavior could also be obtained for these different choices. In view of this, we could keep dephasing and decay rates fixed in Figs. 3 and 4.

In conclusion, we have investigated the controllability of coherent electron population transfer in an asymmetric double QW structure with a common continuum interacting with counterintuitively ordered pulses. Based on the numerical results of the motion equations of element moments, the perfect electron population transfer could be achieved by efficiently optimizing the semiconductor QW structure parameters, such as the direction and the coupling strength of the tunneling from the excited doublet to the common continuum, and the coupling strength of the Fano interference. It is more practical to control the population transfer behavior in the QW systems than in the atomic systems because of its flexible design and the controllable interference strength.

Acknowledgments

This work is supported by the National Natural Sciences Foundation of China (Grant Nos. 60708008, 10874194, 60978013, 60921004), and the Key Basic Research Foundation of Shanghai (Grant No. 08JC1409702).

-
- [1] K. Bergmann, H. Theuer, and B. W. Shore, *Rev. Mod. Phys.* **70**, 1003 (1998).
 - [2] N. V. Vitanov, M. Fleischhauer, B. W. Shore, and K. Bergmann, *Adv. At., Mol., Opt. Phys.* **46**, 55 (2001).
 - [3] M. Weitz, B. C. Young, and S. Chu, *Phys. Rev. A* **50**, 2438 (1994).
 - [4] A. S. Parkins, P. Marte, P. Zoller, O. Carnal, and H. J. Kimble, *Phys. Rev. A* **51**, 1578 (1995).
 - [5] T. Pellizzari, S. A. Gardiner, J. I. Cirac, and P. Zoller, *Phys. Rev. Lett.* **75**, 3788 (1995).
 - [6] U. Gaubatz, P. Rudecki, M. Becker, S. Schiemann, M. Kulz, and K. Bergmann, *Chem. Phys. Lett.* **149**, 463 (1988).
 - [7] C. E. Carroll and F. T. Hioe, *Phys. Rev. Lett.* **68**, 3523 (1992); *Phys. Rev. A* **47**, 571 (1993).
 - [8] E. Paspalakis, M. Protopapas, and P. L. Knight, *Opt. Commun.* **142**, 34 (1997); *J. Phys. B* **31**, 775 (1998).
 - [9] R. G. Unanyan, N. V. Vitanov, B. W. Shore, and K. Bergmann, *Phys. Rev. A* **61**, 043408 (2000).
 - [10] R. Binder and M. Lindberg, *Phys. Rev. Lett.* **81**, 1477 (1998).
 - [11] U. Hohenester, F. Troiani, E. Molinari, G. Panzarini, and C. Macchiavello, *Appl. Phys. Lett.* **77**, 1864 (2000).
 - [12] S. G. Kosionis, A. F. Terzis, and E. Paspalakis, *Phys. Rev. B* **75**, 193305 (2007).
 - [13] H. Y. Hui and R. B. Liu, *Phys. Rev. B* **78**, 155315 (2008).
 - [14] M. C. Phillips, H. L. Wang, I. Rumyantsev, N. H. Kwong, R. Takayama, and R. Binder, *Phys. Rev. Lett.* **91**, 183602 (2003).
 - [15] H. Schmidt, K. L. Campman, A. C. Gossard, and A. Imamođlu, *Appl. Phys. Lett.* **70**, 3455 (1997).
 - [16] H. Sun, S. Q. Gong, Y. P. Niu, S. Q. Jin, R. X. Li, and Z. Z. Xu, *Phys. Rev. B* **74**, 155314 (2006).
 - [17] H. Sun, Y. P. Niu, R. X. Li, S. Q. Jin, and S. Q. Gong, *Opt. Lett.* **32**, 2475 (2007).
 - [18] J. H. Wu, J. Y. Gao, J. H. Xu, L. Silvestri, M. Artoni, G. C. La Rocca, and F. Bassani, *Phys. Rev. Lett.* **95**, 057401 (2005).
 - [19] X. X. Yang, Z. W. Li, and Y. Wu, *Phys. Lett. A* **340**, 320 (2005).
 - [20] E. Paspalakis, M. Tsousidou and A. F. Terzis, *J. Appl. Phys.* **100**, 044312 (2006).
 - [21] J. F. Dynes, M. D. Frogley, J. Rodger, and C. C. Phillips, *Phys. Rev. B* **72**, 085323 (2005).
 - [22] S. Y. Zhu and M. O. Scully, *Phys. Rev. Lett.* **76**, 388 (1996).
 - [23] E. Paspalakis and P. L. Knight, *Phys. Rev. Lett.* **81**, 293 (1998).
 - [24] F. L. Li and S. Y. Zhu, *Phys. Rev. A* **59**, 2330 (1999).
 - [25] S. Q. Jin, S. Q. Gong, R. X. Li, and Z. Z. Xu, *Phys. Rev. A* **69**, 023408 (2004).
 - [26] X. H. Yang and S. Y. Zhu, *Phys. Rev. A* **77**, 063822 (2008).
 - [27] U. Fano, *Phys. Rev.* **124**, 1866 (1961).
 - [28] J. Faist, C. Sirtori, F. Capasso, S.-N. G. Chu, L. N. Pfeiffer, and K. W. West, *Opt. Lett.* **21**, 985 (1996).
 - [29] J. Faist, F. Capasso, C. Sirtori, K. W. West, and L. N. Pfeiffer, *Nature* **390**, 589 (1997).
 - [30] S. E. Harris, *Phys. Rev. Lett.* **62**, 1033 (1989).